The eukaryotic translation initiation factor eIF4E elevates steady-state m^{7}G capping of coding and noncoding transcripts

Biljana Culjkovic-Kraljacic[a], Lucy Skrabanek[b], Maria V. Revuelta[c], Jadwiga Gasiorek[a], Victoria H. Cowling[d], Leandro Cerchietti[c], and Katherine L. B. Borden[a,1]

[a]Institute of Research in Immunology and Cancer, Department of Pathology and Cell Biology, Université de Montréal, Montréal, QC H3T 1J4, Canada; [b]Applied Bioinformatics Core, Department of Physiology and Biophysics, Weill Cornell Medicine, New York, NY 10065; [c]Division of Hematology & Medical Oncology, Department of Medicine, Weill Cornell Medicine, New York, NY 10065; and [d]Centre for Gene Regulation and Expression, School of Life Sciences, University of Dundee, Dundee DD1 5EH, United Kingdom

Edited by Lynne E. Maquat, University of Rochester School of Medicine and Dentistry, Rochester, NY, and approved September 3, 2020 (received for review February 6, 2020)

Methyl-7-guanosine (m^{7}G) "capping" of coding and some noncoding RNAs is critical for their maturation and subsequent activity. Here, we discovered that eukaryotic translation initiation factor 4E (eIF4E), itself a cap-binding protein, drives the expression of the capping machinery and increased capping efficiency of ∼100 coding and noncoding RNAs. To quantify this, we developed enzymatic (cap quantification; CapQ) and quantitative cap immunoprecipitation (CapIP) methods. The CapQ method has the further advantage that it captures information about capping status independent of the type of 5′ cap, i.e., it is not restricted to informing on m^{7}G caps. These methodological advances led to unanticipated revelations: 1) Many RNA populations are inefficiently capped at steady state (∼30 to 50%), and eIF4E overexpression increased this to ∼60 to 100%, depending on the RNA; 2) eIF4E physically associates with noncoding RNAs in the nucleus; and 3) approximately half of eIF4E-capping targets identified are noncoding RNAs. eIF4E's association with noncoding RNAs strongly positions it to act beyond translation. Coding and noncoding capping targets have activities that influence survival, cell morphology, and cell-to-cell interaction. Given that RNA export and translation machineries typically utilize capped RNA substrates, capping regulation provides means to titrate the protein-coding capacity of the transcriptome and, for noncoding RNAs, to regulate their activities. We also discovered a cap sensitivity element (CapSE) which conferred eIF4E-dependent capping sensitivity. Finally, we observed elevated capping for specific RNAs in high-eIF4E leukemia specimens, supporting a role for cap dysregulation in malignancy. In all, levels of capping RNAs can be regulated by eIF4E.

eIF4E | RNMT | methyl-7-guanosine cap | RNA capping

RNA metabolism is a central feature of gene expression and can be used by the cell to modify the proteome after transcription. One of the defining modifications that transcripts undergo is the addition of the methyl-7-guanosine (m^{7}G) "cap" on their 5′ ends. m^{7}G capping status of transcripts impacts their processing, nuclear export, and translation (1). In humans, capping is a three-step process involving RNGTT (RNA guanylyl transferase and 5′ triphosphatase) and RNMT (RNA guanine-7-methyltransferase) (2). RNGTT removes the 5′ gamma-phosphate of the pre-messenger RNA (pre-mRNA) and adds a guanosine via a distinct 5′–5′ pyrophosphate linkage (2). This cap guanylate is methylated by RNMT (1). RNMT contains a conserved methyltransferase domain and utilizes *S*-adenosyl methionine as its methyl donor (1, 3–5). RNMT-activating miniprotein (RAM), a small protein cofactor, binds RNMT and enhances its methylation activity (3, 6, 7). Both RNGTT and RNMT are required for cell survival, highlighting the importance of RNA capping (4, 8–10).

It is often considered that capping of transcripts is restricted to the nucleus, and is a constitutive, cotranscriptional event. In this model, decapping is irreversible and leads to decay. Recent data point to a more dynamic role for capping and, indeed, a model of cap homeostasis has emerged (11). For instance, in the cytoplasm, transcripts can be recapped after decapping using cytoplasmic RNGTT, RNMT, and RAM (11–13). Further, it became evident that mammalian cells express several decapping enzymes which demonstrate selectivity in terms of RNA targets. Importantly, some decapping enzymes hydrolyze cap structures to produce 5′ dephosphorylated RNA products which are not targets of 5′ end decay and could be substrates for recapping (14). Furthermore, decapping enzymes as well as the capping machinery are found in the cytoplasm and nucleus (9, 11–16). These observations suggest two forms of capping: cotranscriptional and posttranscriptional. This parallels 3′ end processing and splicing, both of which can also take place co- and posttranscriptionally (17–19).

Previous studies suggested that capping can be modulated by the transcription factor Myc. Myc overexpression led to increased levels of RNMT which correlated with increased capping of specific transcripts (20). Interestingly, mutations in Myc that disabled transcription did not impair capping (21). Overexpression of Myc increased capping (∼3- to 10-fold) of several of its

Significance

Methyl-7-guanosine (m^{7}G) "cap" addition on 5′ ends of RNA impacts virtually all levels of processing. Titrating capping of transcripts impacts on protein-coding capacity and, for noncoding RNAs, biochemical activity. Capping is widely considered a constitutive housekeeping activity with the expectation that ∼100% of transcripts will be capped at steady state. We developed two methods to quantify capping: quantitative CapIP and an enzymatic method, CapQ. Strikingly, steady-state RNA capping ranged from ∼30 to 50%, much lower than anticipated. eIF4E, a cap-binding protein implicated in human malignancy, elevated capping to ∼60 to 100% for selected transcripts, many of which act in cancer. Indeed, capping is elevated in high-eIF4E primary human cancer specimens. Thus, capping is a significant regulatory step in RNA metabolism.

Author contributions: B.C.-K., L.S., M.V.R., L.C., and K.L.B.B. designed research; B.C.-K., L.S., M.V.R., and J.G. performed research; B.C.-K., L.S., M.V.R., and V.H.C. contributed new reagents/analytic tools; B.C.-K., L.S., M.V.R., L.C., and K.L.B.B. analyzed data; and B.C.-K., L.S., M.V.R., V.H.C., L.C., and K.L.B.B. wrote the paper.

The authors declare no competing interest.

This article is a PNAS Direct Submission.

[1]To whom correspondence may be addressed. Email: katherine.borden@umontreal.ca.

This article contains supporting information online at https://www.pnas.org/lookup/suppl/doi:10.1073/pnas.2002360117/-/DCSupplemental.

First published October 14, 2020.

transcriptional targets such as *CCND1*, *Fbl*, *eIF2B1*, and *eIF4A1* (22). Moreover, RNMT overexpression alone was sufficient to increase capping efficiency of *CCND1* transcripts by ∼3-fold and this correlated with increased protein levels with no changes in total mRNA levels (23). RNMT overexpression transformed immortalized human mammary cell lines, consistent with its effects on specific transcripts such as *CCND1* and *Myc* (23, 24), suggesting that cap regulation could have important biological impacts. Little information is available in terms of understanding the factors that control the production of the capping machinery. Further, technical limitations of current cap immunoprecipitation (CapIP) strategies have not allowed quantification of the percent of transcripts that are capped, knowledge of which is critical for establishing the extent of baseline capping and the extent by which this can be modulated in response to certain stimuli.

Here, we investigated whether one of the major cap-binding proteins in the cell, the eukaryotic translation initiation factor 4E (eIF4E), also played a role in the capping process. eIF4E is found in both the nucleus and cytoplasm (25–29). In the cytoplasm, eIF4E binds the m^7G cap of transcripts and enhances the translational efficiency of a subset of mRNAs with highly structured 5′ untranslated regions (UTRs) (30, 31). In the nucleus, eIF4E binds the m^7G cap of transcripts which contain an ∼50-nt element known as the eIF4E sensitivity element (4ESE) and promotes their nuclear export (32, 33). eIF4E forms an RNA export complex with LRPPRC, which directly binds the target 4ESE RNA, eIF4E, and the exporter CRM1 (34, 35). While characterizing the population of RNAs that are nuclear export targets of eIF4E, we unexpectedly unearthed the principal components of the capping machinery and explore the subsequent impact of eIF4E on capping here.

Results

eIF4E Drives Expression of the Capping Machinery. In order to identify previously unknown eIF4E target transcripts, we leveraged a fundamental difference in the RNA-binding properties of eIF4E in the nucleus and cytoplasm. In the nucleus, eIF4E binds ∼3,000 capped mRNAs which typically are its export targets (36). By contrast, in the cytoplasm, eIF4E binds the majority of capped mRNAs regardless of whether eIF4E enhances their translation efficiency (28, 32, 36–38). Thus, the identification of eIF4E-bound transcripts from the nucleus provides a straightforward strategy for the discovery of target RNAs. Using this strategy, we identified *RNMT*, *RNGTT*, and *RAM* transcripts as nuclear targets of eIF4E.

Specifically, we generated stable U2Os cell lines overexpressing eIF4E (eIF4E-Flag) and corresponding vector controls. For all our studies, three different stable cell lines per condition were assessed to account for biological variability. First, we carried out eIF4E RNA immunoprecipitations (RIPs) from the cross-linked nuclear lysates of vector control U2Os cells to monitor the association of endogenous eIF4E with transcripts. The enrichment of RNAs in the eIF4E RIP versus input RNAs was monitored by qRT-PCR. Relative to nuclear input, endogenous eIF4E binds *RNMT* (∼4.5-fold), *RAM* (∼3.5-fold), and *RNGTT* RNAs (∼3.5-fold) as well as positive controls *Myc*, *Mcl1*, and *CCND1* (∼2.5-, 3.5-, and 2.5-fold, respectively) but not negative control transcripts such as *ACTB*, *POLR2A*, *GAPDH*, or 18S ribosomal RNA (rRNA) (Fig. 1*A*). eIF4E RIPs in eIF4E-Flag cells yielded concordant results with endogenous eIF4E studies (*SI Appendix*, Fig. S1*A*). We obtained similar results using two different eIF4E antibodies (polyclonal rabbit or monoclonal mouse), supporting the robustness of this method (*SI Appendix*, Fig. S1 *B* and *C*).

The association of eIF4E with RNAs encoding the capping machinery in the nucleus raised the possibility that eIF4E increased their nuclear export. Thus, we carried out RNA export assays by assessing target transcript levels in nuclear and cytoplasmic compartments from wild-type eIF4E-Flag, the eIF4E mutant S53A-Flag [active in translation but not in mRNA export or oncogenic transformation (38)], and vector control U2Os cell lines. Fraction quality for export assays was determined using U6 small nuclear RNA (snRNA) for nuclear and transfer RNA for methionine ($tRNA^{Met}$) for cytoplasmic fractions (*SI Appendix*, Fig. S1*F*). Overexpression of wild-type eIF4E increased RNA export by ∼2- to 2.5-fold for *RNMT*, *RAM*, and *RNGTT* as well as *Myc*-, *CCND1*-, and *Mcl1*-positive controls but not the negative controls *ACTB*, *POLR2A*, or *GAPDH* (Fig. 1*B*). eIF4E overexpression did not alter the levels of total transcript examined (*SI Appendix*, Fig. S1*D*). Importantly, there was no increase in export of any transcripts examined in the S53A-Flag cells (Fig. 1*B*), consistent with its export-deficient phenotype (38). Thus, *RNMT*, *RAM*, and *RNGTT* are indeed eIF4E-dependent nuclear export targets.

Next, we investigated whether eIF4E modified the translation efficiency of these RNAs using polysome loading assays in stable eIF4E-Flag and vector control U2Os cells. Importantly, there was no difference between eIF4E and vector cells with regard to the overall polysome profile (*SI Appendix*, Fig. S1*H*), consistent with previous reports (29, 36, 39). For the qRT-PCR analysis, polysome loading experiments were normalized to total RNA in the gradient so that the total area under the curves is 100% for both eIF4E and vector with the relative distribution shown. eIF4E overexpression was associated with a shift of *RNMT*, *RNGTT*, and positive control *VEGF* transcripts to heavier polysome fractions consistent with these being translation targets of eIF4E. By contrast, loading of *RAM* was not increased by eIF4E overexpression, indicating that this transcript was not a translation target of eIF4E (Fig. 1*C*). Examination of the 5′ UTRs (40, 41) indicated that RAM contained motifs that were absent (or less abundant) in RNMT and RNGTT such as RPS3-, RMX-, and YBX1-binding elements suggestive of a molecular basis for their differential translational regulation.

Finally, we investigated the effects of modulating eIF4E expression on the protein levels of the capping machinery (Fig. 1*D*). Our studies demonstrated that eIF4E elevated RNMT, RNGTT, and RAM protein levels whereas the export-deficient mutant S53A only slightly increased levels of Mcl1, Myc, RNMT, and RNGTT (which are both export and translation targets of eIF4E) and did not increase levels of RAM or CCND1 (which are only export targets of eIF4E), consistent with these latter transcripts not being translation targets of eIF4E, as shown by the polysome loading experiments (Fig. 1*C*) (29). In all, eIF4E stimulates the nuclear export of *RNMT*, *RAM*, and *RNGTT* RNAs and, additionally, the translation of *RNMT* and *RNGTT*.

To monitor the effect of eIF4E reduction on levels of the capping machinery, we generated stable U2Os cell lines using CRISPR (CRISPR-4E), and CRISPR control cell lines (CRISPR-Ctrl [control]) using single-guide RNA for the Azami-green fluorescent protein (from *Galaxeidae* coral). Three different stable U2Os cell lines for CRISPR-Ctrl and CRISPR-4E were analyzed. We note that CRISPR-4E depletion led to heterozygous cells, consistent with the complete depletion being lethal. In CRISPR-4E cell lines, nuclear export and corresponding protein levels of the capping machinery were reduced (Fig. 1 *E* and *F*) compared with CRISPR-Ctrl cells, as was the case for positive controls *CCND1*, *Mcl1*, and *Myc*. Reduction in eIF4E did not change levels of total RNAs examined (*SI Appendix*, Fig. S1*E*) and did not alter nontargets such as *ACTB*, *GAPDH*, or *POLR2A* (Fig. 1*E*). In summary, eIF4E elevation stimulated production of the capping machinery while eF4E reduction lowered these levels.

eIF4E Increased Global Levels of m^7G-Capped RNAs. Given eIF4E directly modulated the expression of the capping machinery, we investigated whether eIF4E modulated capping of bulk RNA using immunoblots. To ensure the m^7G cap antibody was specific, we performed dot blots using uncapped and GpppG-capped in vitro transcribed *Luciferase* RNA as negative controls and

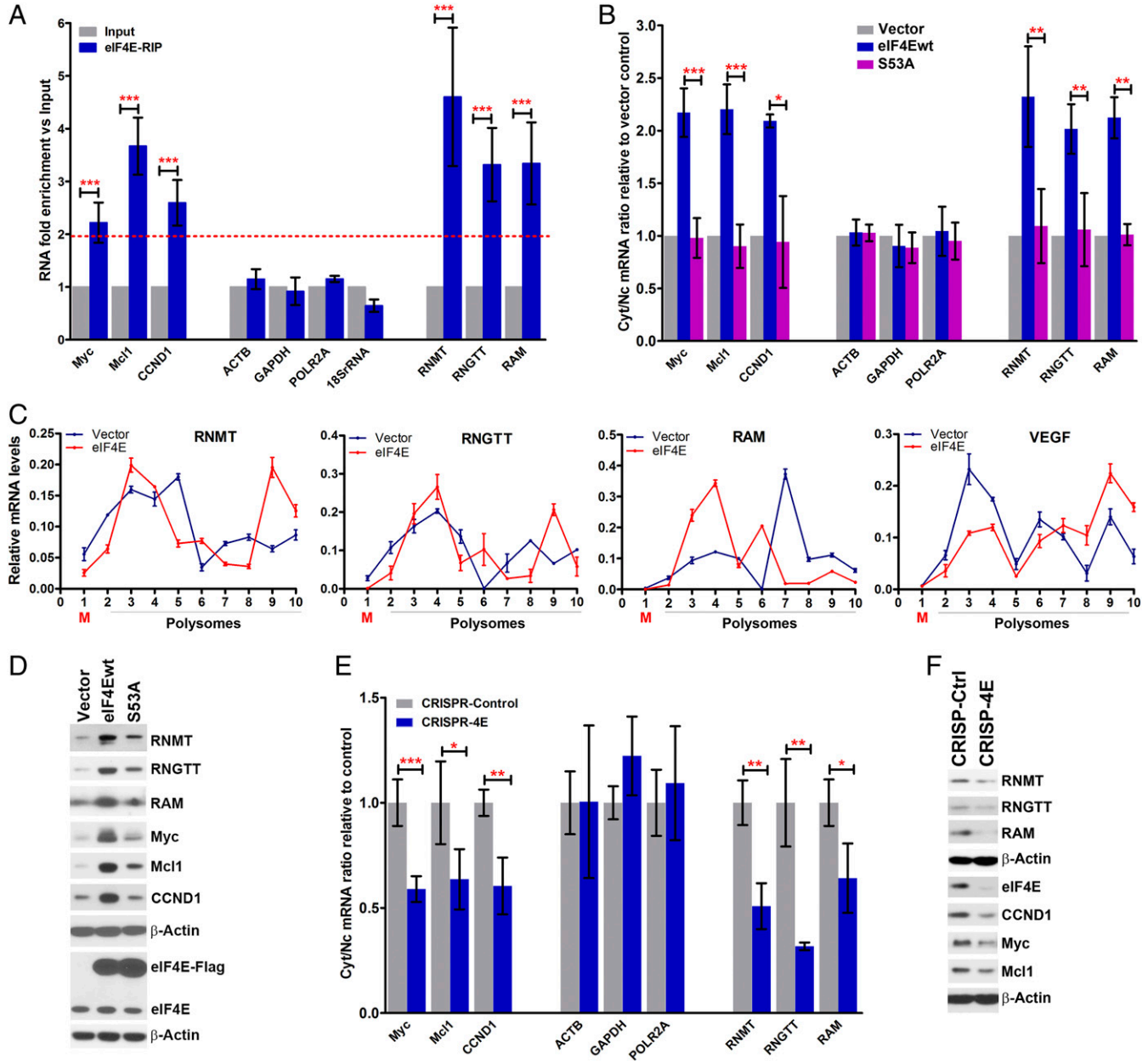

Fig. 1. eIF4E increases expression of the capping machinery. (*A*) The enrichment of mRNAs in eIF4E RIPs versus input RNAs from the nuclear fractions of vector control U2Os cells monitored by qRT-PCR. Data were normalized to input samples and are presented as a fold change. The means, SDs, and *P* values (from Student's *t* test, $*P < 0.05$, $**P < 0.01$, $***P < 0.001$) were derived from five independent experiments (each carried out in triplicate). *Myc*, *Mcl1*, and *CCND1* are known eIF4E nuclear targets and served as positive controls, while *ACTB*, *GAPDH*, *POLR2A*, and 18S rRNA were negative controls. (*B*) RNA export assays for eIF4E-Flag wild-type (eIF4Ewt), S53A mutant-expressing, and vector control U2Os cell lines. RNA export assays were carried out by assessing target transcript levels in nuclear (Nc) and cytoplasmic (Cyt) compartments by qRT-PCR. Data were normalized to vector control to calculate fold change. The means, SDs, and *P* values were derived from three independent experiments (each carried out in triplicate). *P* values between eIF4Ewt and S53A mutant-overexpressing cells are shown. (*C*) Polysome profiling of RNAs encoding the capping machinery in eIF4E-Flag and vector control U2Os cell lines. RNA contents of individual fractions are displayed as a percentage of the given fraction compared with RNA content in the entire gradient for each transcript analyzed. *VEGF* served as a positive control. Experiments were carried out three independent times, and one representative experiment is shown. M, monosome fraction. (*D*) Western blot (WB) analysis of eIF4Ewt, eIF4E mutant S53A-Flag (S53A), and vector control (vector) U2Os cell lines. Myc, Mcl1, and CCND1 served as positive controls. ACTB is a loading control. Both eIF4E-Flag and endogenous eIF4E are shown. Each ACTB blot corresponds to the series of blots above it. Experiments were carried out at least three independent times, and one representative experiment is shown. (*E*) mRNA export assays for CRISPR-4E and CRISPR-Ctrl cell lines, carried out as in *B*. Data were normalized to the CRISPR-Ctrl cell line and presented as a fold change. The means, SDs, and *P* values were derived from three independent experiments (each carried out in technical triplicate). (*F*) WB analysis of capping machinery as a function of eIF4E reduction using CRISPR-4E and CRISPR-Ctrl cell lines. Myc, Mcl1, and CCND1 served as positive controls, while ACTB was used as a loading control. Each ACTB blot corresponds to the series of blots above it. Experiments were carried out at least three independent times, and one representative experiment is shown.

m^7G-capped *Luciferase* RNA (generated via *Vaccinia* capping enzyme) as a positive control. The m^7G cap antibody readily detected m^7G-capped *Luciferase* RNA but did not detect the same amount of uncapped and GpppG-capped *Luciferase* RNAs (Fig. 2*A*). Next, we quantified global m^7G cap levels in total RNAs isolated from three biological replicates of eIF4E-Flag, S53A-Flag, or vector control cells using dot blots. Global m^7G cap levels were elevated ∼2-fold in eIF4E-Flag cells relative to vector

controls (Fig. 2*B*), consistent with its effects on the capping machinery. By comparison, the S53A-Flag cells had global m^7G cap levels similar to vector controls, as expected given its minimal effects on the capping machinery (Fig. 2*B*).

Next, we assessed whether increased levels of the capping machinery were required for eIF4E-dependent capping. As an exemplar, we reduced RNMT protein levels using small interfering RNA (siRNA) and assessed dot blots relative to siRNA controls

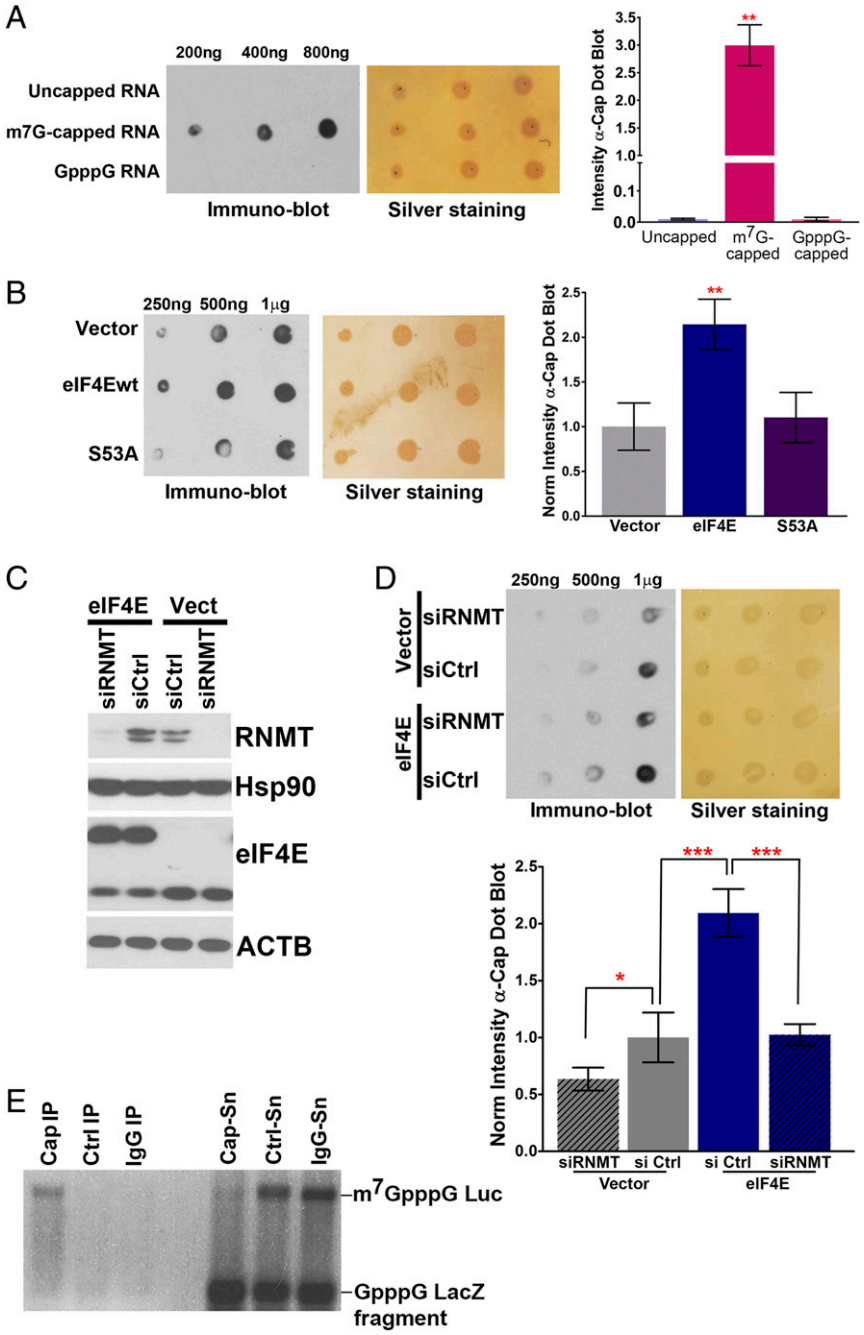

Fig. 2. eIF4E increases m^7G RNA capping. (*A*) Dot blot demonstrating the specificity of the anti-m^7G cap antibody. Immunoblots with the indicated loading of in vitro transcribed uncapped, m^7GpppG-capped, or GpppG-capped *Luciferase* RNAs (*Left*), silver-stained membranes to monitor sample loading (*Middle*), and quantification (*Right*) are shown. (*B*) eIF4Ewt but not the S53A mutant increased m^7G cap levels as observed by immunoblot analysis using the m^7G cap antibody (*Left*), silver-stained membrane for loading (*Middle*), and quantification (*Right*). Quantification is represented as a fold change relative to the vector control, derived from three independent experiments. Means and SDs are shown. (*C*) RNMT is required for eIF4E-dependent increases in m^7G cap levels as assessed by siRNA-mediated knockdown of RNMT. eIF4E and vector control (Vect) U2Os cell lines were transfected with control (Ctrl) or RNMT siRNAs. RNMT knockdown was confirmed by WB and ACTB and Hsp90 were used as loading controls. Both eIF4E-Flag and endogenous eIF4E are shown and neither was altered by RNMT knockdown. Experiments were carried out at least three independent times, and one representative WB is shown. (*D*) Dot blot analysis using the anti-m^7G cap antibody for RNAs isolated from vector control or eIF4E-Flag cells transfected with siCtrl or siRNMT. Dot blots are as in *B*. (*E*) m^7G cap antibody is specific in CapIPs. Agarose gel of RNAs isolated from CapIP, IgGIP, CtrlIP (m^7G cap antibody with an excess of m^7GpppG), and corresponding supernatants (Cap-Sn, IgG-Sn, and Ctrl-Sn) on in vitro transcribed m^7GpppG-capped *Luciferase* or GpppG-capped *LacZ* RNAs. *P* values are from Student's *t* test (*$P < 0.05$, **$P < 0.01$, ***$P < 0.001$).

in eIF4E-Flag cells. RNMT protein levels were reduced substantially in siRNMT cells relative to siCtrls and eIF4E protein levels were not altered (Fig. 2*C*). Moreover, there was a substantial reduction in m^7G cap levels in dot blots (~2-fold) relative to siRNA controls, despite eIF4E overexpression (Fig. 2*D*). Further, siRNMT reduced m^7G levels in vector controls relative to siCtrls. Thus, eIF4E-dependent elevation of m^7G levels required RNMT.

Compartmentalization of eIF4E-Dependent Capping. We investigated whether eIF4E modulated capping in the nuclear and/or cytoplasmic compartments. Quality of cell fractionation was assessed using $tRNA^{Met}$ and U6 snRNA as markers of the cytoplasmic and nuclear compartments, respectively (33, 36). Dot blots indicated that m^7G levels were elevated for eIF4E-Flag cells in both compartments relative to vector controls or S53A-Flag cells (*SI Appendix*, Fig. S2 *A* and *B*). The fold change for each compartment was ~2-fold. Thus, eIF4E impacted global m^7G cap levels in both compartments.

eIF4E Increased Capping Efficiency of Specific Transcripts. To ascertain whether the effects of eIF4E on capping were global or restricted to specific RNAs, we employed an m^7G cap antibody IP (CapIP) strategy and monitored candidate RNAs by qRT-PCR. For these experiments, purified RNAs were used to ensure that the abundance of transcripts in the CapIP was not affected by associated proteins as described (20, 22, 23). Further, RNAs were denatured prior to the CapIP step to eliminate structures that might interfere with the association of the m^7G cap with the cap antibody. Importantly, to obtain the most complete snapshot possible, total RNA was assayed, that is, transcripts were not polyA-selected.

To develop a quantitative CapIP strategy, we carried out a series of experiments to ensure that CapIPs were both quantitative and specific. We first validated the specificity of the CapIP conditions using GpppG-capped *LacZ* or m^7G-capped *Luciferase* RNAs generated by in vitro transcription. After immunoprecipitation, RNAs were extracted and analyzed by agarose gel electrophoresis (Fig. 2*E*). We observed that GpppG-*LacZ* RNAs were at background levels in CapIPs and control immunoglobulin G (IgG) IPs but were readily observed in the supernatant fractions. By contrast, m^7G-*Luciferase* RNAs were observed in the CapIP sample and depleted from the CapIP supernatant fraction (Cap-Sn); furthermore, they were not observed in the IgG control but were present in the IgG supernatant fraction. In parallel, an additional control CapIP in the presence of 100 μM m^7GpppG was conducted to further validate antibody specificity (referred to as the CtrlIP). For this control, we observed the same results as for IgG IP: Both RNAs were absent from CtrlIPs but present in their corresponding supernatant fraction. This is consistent with our findings using immunoblot strategies and indicates that this antibody is indeed specific for m^7G caps in immunoprecipitations.

To determine conditions that were quantitative, we performed titrations with different ratios of m^7G cap antibody to RNAs isolated from eIF4E-overexpressing cells to ensure maximal capture of transcripts in the CapIP. Enrichment of transcripts bound to the cap antibody versus the same condition using mouse IgG was assessed by qRT-PCR (*SI Appendix*, Fig. S2*C*). For the same samples, levels of RNAs in the corresponding Cap-Sn fractions were monitored (*SI Appendix*, Fig. S2*D*). *CCND1* and *Myc* RNAs were followed since they are both established RNMT-capping targets (6, 23), as well as negative controls *ACTB* and *GAPDH*. We found that the ratio of 5 μg of cap antibody to 4 μg of RNA was optimal, since further increase in the amount of antibody did not enrich RNAs in the CapIPs nor did it decrease levels of unbound RNAs in the Cap-Sn fractions as compared with 10 μg of antibody and 4 μg of RNA (*SI Appendix*, Fig. S2 *C* and *D*).

As a final validation step, we examined the ability of m^7GpppG or GpppG to compete for RNAs bound in the CapIPs using RNAs isolated from eIF4E-Flag cells (*SI Appendix*, Fig. S2*E*). Incubation with m^7GpppG depleted *Myc* and *CCND1* RNAs from CapIP by ~10-fold whereas GpppG (which is not methylated but contains the pyrophosphate linkage) did not compete. m^7GpppG treatment similarly reduced the levels of other RNAs in the CapIP such as *Mdm2* (~5-fold), *POLR2A* (~10-fold), and *ACTB* and *GAPDH* (~3-fold). Given these findings, we integrated a separate control reaction using m^7GpppG competition into our experimental design (*SI Appendix*, Fig. S2*F*). In these CtrlIPs, as described above, RNAs were incubated simultaneously with the cap antibody and 100 μM m^7GpppG to determine the extent of nonspecific (i.e., cap-independent) binding of RNAs to the cap antibody or beads (*SI Appendix*, Fig. S2*F*). Indeed, this method was very effective at eliminating background binding of RNAs to the beads (*SI Appendix*, Fig. S2*G*). In this way, the background binding for RNAs could be determined in parallel with the CapIP experiments from the same samples.

With quantitative conditions in hand, we monitored the capping efficiency of selected RNAs in eIF4E-Flag or vector control stable cell lines. Comparison of RNA enrichment in CapIPs normalized to their inputs showed that eIF4E overexpression increased capping of *CCND1* (~3.5-fold) and *Myc* (~3-fold) relative to vector controls (Fig. 3*A*) without altering total RNA levels (*SI Appendix*, Fig. S1*D*). Capping of other eIF4E export targets was similarly elevated, such as *Mcl1* and *Mdm2* RNAs (~3- and ~4-fold, respectively). The capping status of *POLR2A*, *ACTB*, and *GAPDH* was only modestly affected by eIF4E overexpression (<2-fold) and, as such, served as negative controls. Thus, the effects of eIF4E were not global but rather restricted to selected RNAs with increases in the ~2- to 4-fold range, depending on the transcript examined.

CapIP experiments coupled with qRT-PCR detection provided information about alterations in capping but, by its nature, could only provide relative fold change. To truly understand the magnitude of the effects of eIF4E on capping, we designed a strategy to calculate the percentage of capped transcripts for a specific RNA in vector and eIF4E-overexpressing cells. In parallel with the above CapIP experiments, RNAs were isolated from the supernatant fractions of the CapIPs and CtrlIPs, denoted Cap-Sn and Ctrl-Sn reactions, respectively, and analyzed by qRT-PCR (*SI Appendix*, Fig. S2*F*). A ratio of Cap-Sn RNA to Ctrl-Sn RNA provided the percent uncapped, which was then converted to the percent of capped RNA. In all cases, values were normalized to 18S rRNA since it is not subject to capping. Capping percentages of *Myc*, *CCND1*, *Mdm2*, and *Mcl1* were elevated in eIF4E-Flag cells (~30% in vector control cell lines compared with ~60 to 80% in eIF4E-Flag cells), with no detectable changes in capping efficiency for *ACTB*, *GAPDH*, or *POLR2A* RNAs (Fig. 3*B*). These data agreed well with the fold changes observed in the CapIPs for eIF4E versus vector cells, which were in the ~2- to 4-fold range (Fig. 3*A*).

Our previous studies demonstrated that increased expression of RNMT preferentially enhanced steady-state capping of selected transcripts including *RuvBL1*, *eIF4AI*, *eIF2B1*, *CTNNB1*, *CDK2*, *MINA*, and *Fbl*, as well as the long noncoding RNAs (lncRNAs) *MALAT1* and *NEAT* (6, 7, 22, 23, 42). Given that eIF4E stimulated RNMT production and these latter transcripts were RNMT targets, we reasoned these would also be eIF4E-dependent capping targets. Indeed, all of these RNAs had increased enrichment in CapIPs (~2- to 4-fold) and increased capping percentages as derived from Cap-Sn analysis (from 20 to 40%, to 60 to 90%) in eIF4E-Flag cells relative to vector cells (Fig. 3 *A* and *B*). For comparison, we examined two transcripts which were not RNMT-capping targets, *CDK4* and *Cdc25A* (6, 7, 22, 23, 42). Consistently, we observed no alteration to capping for these transcripts in eIF4E-Flag cells relative to vector controls. Thus, eIF4E overexpression increased capping percentages

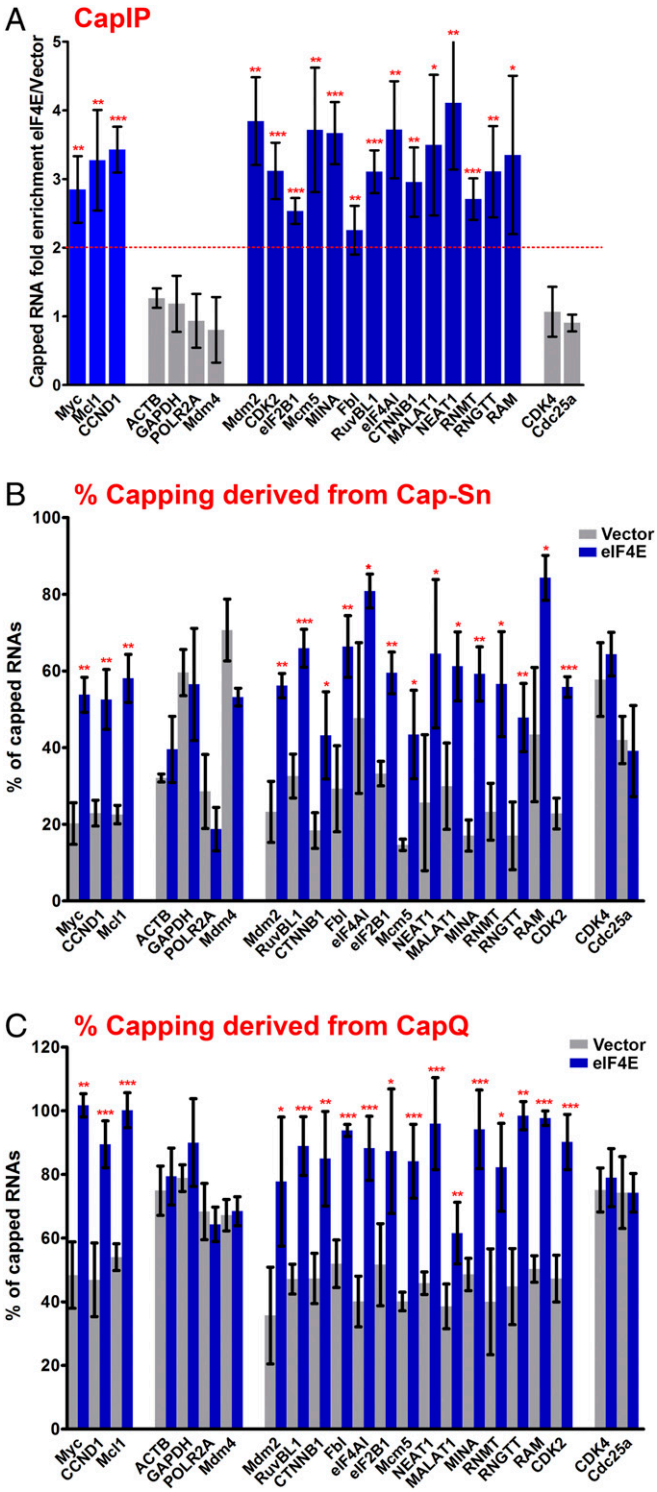

Fig. 3. eIF4E increases capping percentages for specific RNAs. (*A*) Fold enrichment of RNAs in CapIPs from eIF4E-Flag relative to vector control U2Os cells by qRT-PCR. Data were first normalized to input and antibody control (m^7G cap antibody with excess of m^7GpppG; CtrlIP) samples for each vector and eIF4E set. Then, values were normalized to vector and presented as a fold change for each RNA. The means, SDs, and *P* values (from Student's *t* test, $*P < 0.05$, $**P < 0.01$, $***P < 0.001$) derived from three independent experiments (each carried out in triplicate) are shown. (*B*) Percentage of capped transcripts derived from the levels of transcripts in supernatant fractions after CapIPs (Cap-Sn) assessed by qRT-PCR. All samples were normalized to 18S rRNA, which is not m^7G-capped, and the ratio of Cap-Sn RNA to Ctrl-Sn RNA levels provided the percent of uncapped RNA in the Cap-Sn, which was then converted to the percent of capped RNA. The means, SDs, and *P* values were derived from three independent experiments (each carried out in triplicate). (*C*) Percentage capping derived from CapQ. Percentage of capping was calculated as outlined in the text. The means, SDs, and *P* values were derived from three independent experiments (each carried out in triplicate).

of a specific subset of RNAs, which included protein-coding and noncoding transcripts.

Enzyme-Based Capping Analysis: Cap Quantification. To ensure our results were antibody-independent, we developed an enzymatic method to measure capping efficiency which we refer to as cap quantification (CapQ). This method exploits differential sensitivity of capped and uncapped RNAs to tobacco acid pyrophosphatase (TAP) and alkaline phosphatase (AP) (*SI Appendix*, Fig. S3). Specifically, capped RNAs are unaffected by AP whereas their treatment with TAP leaves a 5′ monophosphate on the RNA which is then ligated to RNA oligonucleotides and used for library preparation; the uncapped RNAs will have a 5′ OH group after AP treatment and, thus, will not be affected by TAP nor be ligated to the RNA oligonucleotides. To determine total RNA levels for the same samples, separate aliquots of RNAs were treated with AP followed by polynucleotide kinase (PNK) and TAP. As a result, all RNAs, regardless of their initial 5′ end status, have a single phosphate group which can be used for library preparation (*SI Appendix*, Fig. S3), allowing us to determine total RNA levels from parallel samples. This method is similar to refs. 43 and 44, but proffers certain advantages including measurement of total RNA levels from the same samples, independence with respect to the type of caps, and, finally, permits the calculation of the percentage of capped RNAs.

We assessed the concordance between the CapQ assay and the above quantitative CapIP/Cap-Sn methods examining the same target RNA cohort in vector and eIF4E-Flag cells (Fig. 3*C*). Results obtained from these methods were similar in terms of both relative fold changes and percentages of capped transcripts observed. The pools of eIF4E-dependent target and nontarget RNAs were identical for both methods. Specifically, target RNAs included *CCND1*, *Myc*, *Mdm2*, *Mcl1*, *RuvBL1*, *eIF4AI*, *eIF2B1*, *CTNNB1*, *CDK2*, *Mcm5*, *Fbl*, *MINA*, as well as lncRNAs *NEAT1* and *MALAT* (Fig. 3*C*). Nontarget RNAs also remained the same for both methods, for example *ACTB*, *POLR2A*, *CDK4*, and *Cdc25a*. The capping efficiency of RNAs was increased by ∼2- to 3-fold for target transcripts, ranging from ∼30 to 50% in vector cells to 80 to 100% in eIF4E-Flag cells. Thus, CapIP/Cap-Sn and CapQ analyses both demonstrated that eIF4E substantially increases the percent of capped transcripts for specific pools of RNA.

Both quantitative CapIP/Cap-Sn and CapQ methods yielded lower levels of capping in vector cells than might be anticipated. While antibody issues such as avidity or accessibility could be encountered theoretically in the CapIP/Cap-Sn method, CapQ is independent of these. Since RNAs were denatured prior to either procedure, it is highly unlikely that structured RNA elements would interfere with the accessibility to TAP or the cap antibody. Given the quantitative agreement of our CapQ and CapIP/Cap-Sn methods, it seems likely that the general efficiency of capping of at least a subset of RNAs is significantly lower than constitutive models of capping would suggest but is consistent with dynamic models which include rounds of decapping and recapping (11). We note that CapQ and CapIP/Cap-Sn methods theoretically capture slightly different RNA populations. Cap antibody-based methods will only select m^7G-capped RNAs whereas CapQ methods will capture RNAs with any form of cap with a pyrophosphate linkage including m^7G,

GpppG, and rarer NAD and FAD caps, for example. This could account for the modest differences observed in the percentage of capping derived from these assays. Despite this subtle difference, the RNA populations examined are highly concordant both in identity and the percentage capping.

Identification of eIF4E-Dependent Capping Targets Using CapIP-Seq. We sought to discover additional eIF4E-dependent capping targets. Since CapIP/Cap-Sn and CapQ methods gave highly concordant results, we carried out CapIPs on total RNAs from three different eIF4E-Flag or vector stable cell lines and subjected each to RNA sequencing (RNA-seq). Input samples were also analyzed to assess the impact of eIF4E on total transcript levels. Out of the 58,684 genes annotated by Gencode, 23,283 had at least 10 reads across all input samples, and were included in the differential gene expression analysis. Consistent with its posttranscriptional function, eIF4E overexpression only impacted transcript levels for ∼400 genes (<2%), with only 147 elevated in eIF4E-Flag relative to vector control cells (*SI Appendix*, Table S1). To examine the content in the CapIP in vector versus eIF4E cells, we used the following metric: median transcripts per million minus the median absolute deviation (median[TPM]–MAD). Globally, we observed ∼7,145 transcripts with a score >10 and 1,236 >100 with the majority (∼80%) of transcripts in CapIP-seq with a score <1. Thus, while our assay enabled discovery of RNA targets, its overall sensitivity was limited and could not provide a global view of capping. In this way, these data likely underrepresent the number of eIF4E-dependent capping targets but, importantly, provided an opportunity to identify previously unknown targets.

We identified 84 RNAs with increased capping in eIF4E-overexpressing cells versus vector controls and ∼70 transcripts with reduced capping (*SI Appendix*, Fig. S4*A* and Table S2). Interestingly, half of the RNAs with increased eIF4E-dependent capping were noncoding RNAs (43/84), such as lncRNAs, antisense RNAs, and processed pseudogenes (*SI Appendix*, Table S2). This is consistent with our identification of lncRNAs as capping targets of eIF4E above (*MALAT* and *NEAT*; Fig. 3). For transcripts with decreased capping, ∼1/3 of targets were noncoding RNAs (25/70; *SI Appendix*, Table S2). Most noncoding RNAs are processed similar to mRNAs [capped, spliced, and polyadenylated (45–47)] and, thus, capping status would greatly impact on their functionality. We selected nine RNAs to validate using qRT-PCR; this selection was based on whether RNAs were involved in oncogenic processes and designed to probe different RNA classes (coding, lncRNA, pseudogenes, etc.). All nine of these targets, *TGM2*, *PDK1*, *TNFRSF14*, *TNFSF8*, *CFLAR*, *HRNR*, *AC006116.27*, *AC006116.24*, and *ABALON*, were enriched in CapIPs from eIF4E-Flag cells relative to vector controls by qRT-PCR (*SI Appendix*, Fig. S4*B*). Most targets had no change in RNA levels while a few had increased or decreased levels in eIF4E-Flag inputs (*TGM2*, *TNFRSF14*, *CFLAR*, and *ABALON*; *SI Appendix*, Table S1). Importantly, all RNAs from CapIPs were normalized to their respective input transcript levels, and thus the increased capping observed was not a product of increased transcription.

Ingenuity Pathway Analysis of eIF4E-dependent capping targets obtained from CapIP-seq and from our candidate studies above revealed the top "molecular and cellular functions" to be "cell death and survival" (P values ranging from 0.046 to 7×10^{-5}) and "cell morphology" (P values ranging from 0.046 to 0.0002), consistent with functions of eIF4E in cellular remodeling to support an oncogenic phenotype (37) (*SI Appendix*, Fig. S4*C*). Unfortunately, some of the lncRNAs were not annotated and therefore could not be used in this analysis. In all, the transcripts that were enriched in the CapIP of eIF4E-Flag cells included those that encoded oncogenic proteins or were noncoding RNAs with oncogenic activities, which could underpin, at least in part, eIF4E's known biological activities in survival, adhesion, migration, invasion, and metastasis.

eIF4E-Dependent Capping Does Not Rely on Physical Interactions with eIF4E. We next determined whether the association of eIF4E with target RNAs was required for increased capping. We monitored the ability of eIF4E to bind with target transcripts in nuclear and cytoplasmic fractions and compared this association with its capping status as determined by CapIP/Cap-Sn and CapQ experiments (Fig. 3, Table 1, and *SI Appendix*, Figs. S4 and S5). Importantly, we observed that all RNAs examined bound to eIF4E in the cytoplasm, indicating that eIF4E binding alone in the cytoplasm was not predictive of increased capping, for example, both negative controls such as *GAPDH* and capping targets such as *Myc* bound eIF4E in the cytoplasm (Table 1 and *SI Appendix*, Fig. S5*D*). Indeed, these bound both wild-type eIF4E and the S53A mutant there (*SI Appendix*, Fig. S5*D*). In terms of binding eIF4E in the nuclear fraction, we observed some RNAs that associated with nuclear eIF4E that were indeed capping targets (*CCND1* and *Myc*) (*SI Appendix*, Fig. S5 *A* and *B*). No RNAs examined bound to the S53A mutant in the nucleus, consistent with previous studies that this mutant was impaired in binding to RNAs in this fraction (38). Some eIF4E-dependent capping targets did not associate with nuclear wild-type eIF4E (e.g., *RuvBL1*, *CTNNB1*, *Fbl*, *eIF4AI*, *PDK1*, *HNRN*, and *TGM2*; *SI Appendix*, Fig. S5 *A–C*). By contrast, *Mdm4* bound to nuclear eIF4E but was not a capping target; however, *Mdm4* was an RNA export and translation target of eIF4E as demonstrated by RNA export assays and polysome analyses (*SI Appendix*, Fig. S5 *E* and *F*). Taken together, the physical association of eIF4E with RNAs was not a prerequisite for increased capping efficiency (Table 1).

What RNA Elements Confer Capping Selectivity? Given that eIF4E-dependent enhancement of capping did not require its physical association, we postulated that there was a USER code that conferred increased capping. In order to identify this element, we analyzed capping activity of LacZ constructs containing 5′ and 3′ UTR elements derived from the human *CCND1* transcript

Table 1. Some, but not all, capping targets are eIF4E nuclear targets

	Capping CapIP/CapQ	Nc 4E RIP	Cyt 4E RIP
Myc	+/+	+	+
CCND1	+/+	+	+
Mcl1	+/+	+	+
Mdm2	+/+	+	+
RNMT	+/+	+	+
RNGTT	+/+	+	+
RAM	+/+	+	+
eIF4AI	+/+	–	+
CTNNB1	+/+	–	+
Fbl	+/+	–	+
RUVBL1	+/+	–	+
Mdm4	–/–	+	+
ACTB	–/–	–	+
GAPDH	–/–	–	+
POLR2A	–/–	–	+
CDK4	–/–	–	+
Cdc25A	–/–	–	+

Summarized results from CapIP and eIF4E RIP analyses for example RNAs. RNAs with ≥2-fold enrichment in eIF4E RIP (Fig. 1*A* and *SI Appendix*, Figs. S1 *A* and *B* and S5 *A–D*) or for capping ≥2-fold enrichment in CapIPs (Fig. 3) were considered positive targets. Note that for cytoplasmic 4E RIPs, similar results were obtained for both eIF4E and S53A mutant-overexpressing cells (*SI Appendix*, Fig. S5*D*).

CELL BIOLOGY

(Fig. 4*A*). *CCND1* RNA was selected because it is a well-characterized export target of eIF4E and contains an ∼50-nt 4ESE export element in its 3′ UTR (32–34). Moreover, *CCND1* is a target of eIF4E-dependent, as well as RNMT-dependent, capping (Fig. 3) (23). In U2Os cells, *CCND1* is not an eIF4E-dependent translation target (29), limiting its control to the nucleus (29, 32, 33). Full-length and truncated UTRs of *CCND1* RNA were fused to LacZ and capping was assessed by CapIP as a function of eIF4E overexpression (Fig. 4*B*). In parallel, CapIPs in the presence of excess m^7GpppG (CtrlIPs) were conducted to ensure specificity. CapIP values presented are normalized to the corresponding CtrlIP and additionally to total RNA levels for each chimeric construct to control for slight variations in expression of the different constructs. These studies were conducted in eIF4E-Flag cells, to ensure constant levels of RNMT, RNGTT, and RAM.

Using this strategy, we observed that the 5′ UTR of *CCDN1* (includes the 5′ UTR from 1 to 209 and the first coding exon from 210 to 392) and the last ∼1,500 nt of the *CCND1* 3′ UTR (nucleotides 2824 to 4299) were both dispensable for increased capping. The eIF4E-dependent RNA export element, the 4ESE (*CCND1* nucleotides 2481 to 2520), also did not enhance capping. By contrast, the first ∼1,200 nt in the 3′ UTR retained the same capping activity as the full-length 3′ UTR (nucleotides 1611 to 2824; Fig. 4*B*). Further mapping defined an ∼800-nt region (nucleotides 1611 to 2459) which was sufficient for an ∼2.5-fold increase in capping. Additional mapping from the 5′ and 3′ ends of this fragment resulted in a substantial loss of eIF4E-dependent capping activity. This suggests that the cap sensitivity element (CapSE) is composed of structural features that are not colinear. Future studies using methods such as SHAPE and RNase mapping will undoubtedly define a smaller region. However, since fragment 1611 to 2459 recapitulated the activity of the full-length 3′ UTR in terms of eIF4E-dependent capping activity, we denoted it the CapSE. We note that nuclear eIF4E did not bind *LacZ-CapSE* transcripts but did bind the positive control *LacZ-4ESE* RNAs with a >4-fold enrichment (*SI Appendix*, Fig. S6). In this way, the CapSE is physically and functionally independent of the 4ESE.

Given eIF4E did not RIP with *LacZ-CapSE* transcripts, we reasoned that it recruited other factors. We investigated RNMT since its overexpression is associated with increased capping and it binds to RNAs both at the 5′ end to methylate the cap and also the 3′ UTRs of some transcripts (7). We carried out RNMT RIPs of the above *LacZ-CCND1* chimeric constructs in eIF4E-overexpressing cells (so that RNMT levels would remain constant across experiments) and monitored enrichment in these RIPs using qRT-PCR. We observed that the constructs that contain the CapSE, including the smallest CapSE element identified (nucleotides 1611 to 2458), were enriched in the RNMT RIP by over 2-fold relative to either *LacZ* alone or the *LacZ-4ESE* chimeras (Fig. 4*C*). Interestingly, *CCDN1* 5′ UTR-*LacZ* was also enriched in RNMT, but this was not sufficient to increase eIF4E-dependent capping (Fig. 4*B* vs. Fig. 4*C*). In all, the CapSE recruits RNMT, and not eIF4E.

Increased Capping of Selected Transcripts in High-eIF4E Acute Myeloid Leukemia Specimens. We set out to investigate whether eIF4E-dependent capping was increased in cancer by analyzing this activity in high-eIF4E acute myeloid leukemia (AML) primary patient specimens, where eIF4E is highly enriched in the nucleus and characterized by elevated eIF4E-dependent RNA export activity (28, 34, 48). We observed a robust increase in

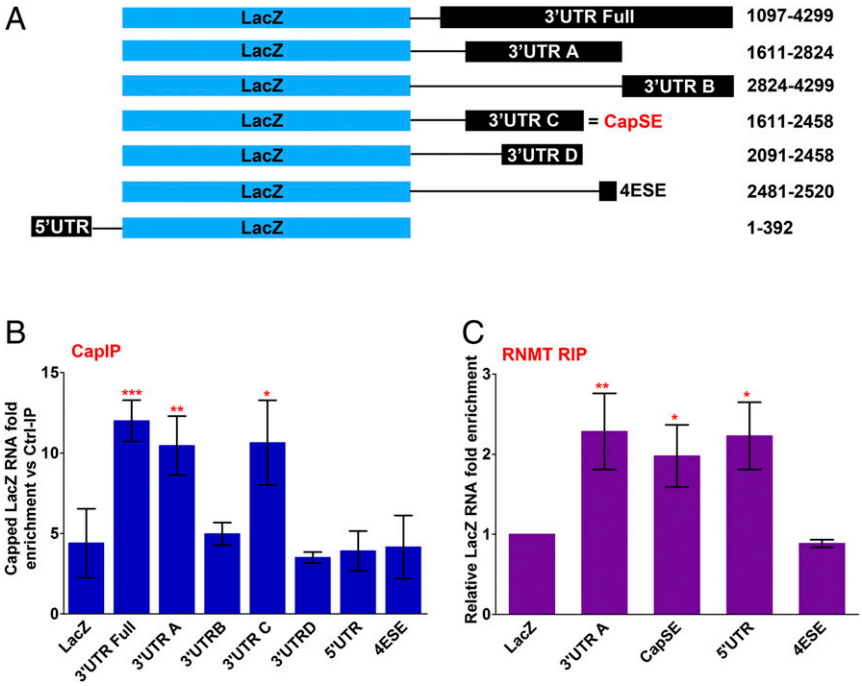

Fig. 4. Determination of an RNA element sufficient to support eIF4E-dependent capping. (*A*) Schematic representation of chimeric constructs used for mapping of CapSE. Full-length 5′ UTR or 3′ UTR constructs of human *CCND1* mRNA were cloned up- or downstream of LacZ, respectively. Numbers represent the position of UTR fragments in *CCND1* mRNA. (*B*) eIF4E-Flag U2Os cells were transiently transfected with LacZ or chimeric LacZ constructs containing the first exon (5′ UTR-LacZ) or indicated 3′ UTR portions of *CCND1*. Total RNAs were used for CapIPs. Data were normalized to input and antibody control (m^7G cap antibody with an excess of m^7GpppG) for each sample, and presented as a fold change for each RNA. The means and SDs derived from three independent experiments (each carried out in triplicate) are shown. (*C*) Nuclear fractions of the indicated cells were immunoprecipitated with an anti-RNMT antibody and IPs were monitored by qRT-PCR. Data were normalized to input samples and presented as a fold change relative to *LacZ*. The means, standard deviations, and *P* values (from Student's *t* test, $*P < 0.05$, $**P < 0.01$, $***P < 0.001$) derived from three independent experiments (each carried out in triplicate) are shown.

RNMT for 20/20 AML specimens examined and similarly for RNGTT protein levels for 8/8 AML specimens that we previously established had highly elevated eIF4E levels relative to four healthy volunteers (Fig. 5*A* and *SI Appendix*, Fig. S7*A*). We note that there is some variation among specimens in terms of the extent of the elevation in both cases. Next, we examined whether capping was elevated in these AML specimens using CapIP and qRT-PCR (total RNAs isolated from four high-eIF4E AML patients and four healthy donors). We observed that capping was elevated (~2-fold) for eIF4E-dependent cap targets such as *Myc*, *Mdm2*, *CDK2*, *Fbl*, *MALAT*, *RuvBL1*, and *CTNNB1* but not for *ACTB*, *POLR2A*, *CDK4*, *Mdm4*, or *Cdc25a* (Fig. 5*B* and *SI Appendix*, Fig. S7*B*). In all, we observed increased steady-state capping for both coding and noncoding RNAs in primary AML specimens.

Discussion

The textbook view of RNA capping has been that it is a constitutive, cotranscriptional process whereby decapping is irreversible and inexorably leads to RNA decay. Our data support the emerging view that capping is dynamic, consistent with the discovery of recapping as well as of incompletely capped RNAs in human cells (11–13, 49–52). We developed the CapQ and quantitative CapIP/Cap-Sn tools to quantify the relative percent capping for specific transcripts. These methodological developments led to the surprising revelation that there are RNA populations not efficiently capped at steady state, with capping percentages as low as ~20 to 30%. Clearly, it is possible that conditions that modulated capping could impact stability. However, 24/32 RNAs identified and validated by qRT-PCR as eIF4E-dependent capping targets had no detectable change in their total RNA levels in vector relative to eIF4E-FLAG cells (*SI Appendix*, Fig. S5*G*). Of the eight remaining, seven had increased RNA levels upon eIF4E overexpression and one had reduced levels. Furthermore, the half-lives of eIF4E-dependent capping targets *CCDN1*, *Myc*, and *Mdm2* RNAs (or indeed of noncapping targets, e.g., *LacZ*/*LacZ-4ESE* or *ACTB*) were not altered upon eIF4E overexpression as assessed by actinomycin D treatment and qRT-PCR (32, 33, 38) despite their elevated capping. Thus, there appears to be no link between eIF4E expression and stability for the RNAs examined. There are possible explanations for our observations. For example, uncapped RNAs or RNAs with immature caps could be sequestered into subcellular structures in order to protect them or another nonmutually exclusive possibility is that there could be factors that bind to and thereby protect these RNAs. These are important future areas to study. Another important mechanistic issue relates to the location and timing of capping and recapping. Recent studies suggested that posttranscriptional recapping occurred in either the nucleus or cytoplasm and could be driven in both compartments by RNGTT, RNMT, and RAM (11–13). Indeed, we observed that eIF4E stimulated capping in both compartments (*SI Appendix*, Fig. S2 *A* and *B*). Determinations of capping efficiency here are all steady-state and thus we cannot disentangle de novo capping from recapping in the nucleus, while in the cytoplasm it is presumably recapping.

Given that eIF4E is a cap-binding protein, increased capping could be a product of protection of the cap from decapping enzymes. However, several lines of evidence reveal that this is not the case. For instance, there was no correlation between transcripts binding to eIF4E in RIPs and increased capping upon eIF4E overexpression. Indeed, all RNAs examined bound to eIF4E in the cytoplasm but not all were capping targets, for example *Mdm4*, *ACTB*, and *GAPDH*. Conversely, some eIF4E-dependent capping targets, such as *RuvBL1*, *CTNNB1*, *Fbl1*, *eIF4A1*, and so forth, did not interact with eIF4E in nuclear RIPs but were eIF4E-dependent capping targets (Table 1 and *SI Appendix*, Fig. S5 *A–D*). Furthermore, *LacZ-4ESE* RNA physically interacted with nuclear eIF4E (32, 33) while *LacZ-CapSE* did not (*SI Appendix*, Fig. S6) but *LacZ-CapSE* has an ~2.5-fold increase in capping upon eIF4E overexpression relative to *LacZ* or *LacZ-4ESE*. Finally, some RNAs found in eIF4E RIPs were also eIF4E-dependent capping targets, such as *CCND1* and *Myc*. Thus, eIF4E binding to RNAs is not required for increased capping nor in the cases when it is observed does it mean an a priori increase in capping. Given that there is not a strong relationship between eIF4E binding and increased capping, it is possible that increased capping permits some RNAs to bind other cap-binding proteins, such as eIF3d, CBC, PARN, and so forth, all of which act in multiple steps in RNA processing including translation (53). In our studies, eIF4E-dependent capping is derived from the ability of eIF4E to drive the expression of the capping machinery via its effects on export and translation of *RNMT*, *RNGTT*, and *RAM*. Consistently, the S53A mutant was impaired in these activities as well as in capping (*SI Appendix*, Fig. S2*A*). Moreover, reduction of RNMT protein levels also impaired eIF4E-dependent capping in eIF4E-overexpressing cells (Fig. 2*D*). Together, these latter points

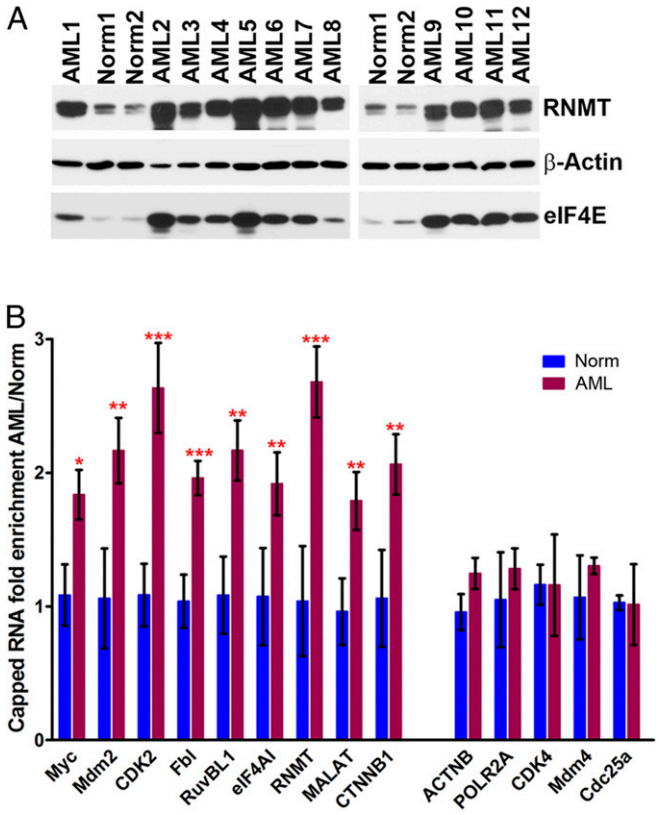

Fig. 5. High-eIF4E AML specimens show increased RNMT protein levels and increased capping of selected transcripts. (*A*) WB analysis of RNMT levels in primary AML samples with high eIF4E levels and bone marrow mononuclear cells from healthy volunteers (Norm, normal). ACTB was used as a loading control. WB analysis for RNGTT is shown in *SI Appendix*, Fig. S7*A*. (*B*) Comparison of RNA enrichment in CapIPs using RNAs isolated from high-eIF4E primary AML cells (four samples) vs. bone marrow mononuclear (three samples) or CD34+ cells (one sample) from healthy volunteers (Norm), monitored by qRT-PCR. CapIPs were first normalized to input for each sample, then grouped and averaged for AML and normal samples, and finally normalized to values obtained for normal samples and presented as a fold change. The means, standard deviations, and *P* values (from Student's *t* test, $*P < 0.05$, $**P < 0.01$, $***P < 0.001$) calculated for AML and normal grouped samples (each carried out in triplicate) are shown. *ACTB*, *POLR2A*, *CDK4*, and *Mdm4* served as negative controls. For the range of differences among AML and normal groups, see *SI Appendix*, Fig. S7*B*.

support a model whereby eIF4E-dependent capping is derived, at least in part, from increasing levels of the capping machinery. eIF4E may impact on capping via additional means; this remains to be explored.

Our studies indicated that the USER codes for eIF4E's activities in translation (complex 5′ UTR) and nuclear export (4ESE) are distinct from the CapSE. The CapSE appears to play a role in RNMT recruitment to the RNA. Future secondary and tertiary structure-based mapping studies will provide a better definition of the CapSE and will allow an exploration into its conservation across eIF4E-dependent capping targets and/or the determination of additional types of CapSE elements. Whether RAM and RNGTT are also recruited by the CapSE remains to be examined but is an important possibility. Most importantly, the CapSE serves as a proof of principle that elements conferring increased capping exist.

Our studies unexpectedly revealed that eIF4E impacted the processing of some noncoding RNAs and, indeed, physically interacted with a subset of these (Table 1 and *SI Appendix*, Fig. S5 *A–C*). Similar to eIF4E, many of these noncoding RNAs are dysregulated in human cancers such as *MALAT1* and *NEAT* (53–55). Like eIF4E, these have been implicated in reduction of apoptosis and increased proliferation and metastasis. Many of the other noncoding RNAs identified are competing endogenous RNAs which act as sponges for tumor suppressive microRNAs. In parallel, many of the coding transcripts identified are similarly implicated in cancer, such as *Mdm2*, *Myc*, *Mcl1*, and *CTNNB1* (29, 32, 33, 37, 56). Some of these RNAs play roles in the same biochemical pathways, such as *CTNNB1* and the lncRNA that protects it [*SLC4O1-AS1* (57)]. In this way, both coding and noncoding RNAs can act as downstream effectors of the oncogenic effects associated with eIF4E. Consistently, we observed that eIF4E-dependent capping is dysregulated in primary high-eIF4E AML specimens. The unanticipated impact of eIF4E on noncoding RNA, which constitutes more than 95% of the transcriptome (58, 59), substantially expands its sphere of influence. Whether eIF4E impacts other aspects of noncoding RNA metabolism will be an important future direction. In all, eIF4E is positioned to modulate the steady-state capping of both coding and noncoding RNAs and as such will impact on their fitness as substrates for multiple steps in RNA metabolism and their ultimate physiological activity.

Materials and Methods

See *SI Appendix* for further information.

Cell Culture, Polysome Profiling, Cellular Fractionation, and RNA Export Assays. U2Os cells (obtained from ATCC) were maintained under standard conditions (for details, see *SI Appendix*) and transient transfection conditions and generation of stable cell lines are described in *SI Appendix*. Polysome profiling, fractionation, and export assays were done as described (36, 37). Detailed protocols are described in *SI Appendix*.

RIP, CapIP, and Cap-Sn. Nuclei isolated using the cellular fractionation protocol were rinsed twice with 1× phosphate-buffered saline (PBS) and fixed with 1% paraformaldehyde for 10 min at room temperature with rotation, quenched 5 min with 0.15 M glycine, washed three times with 1× PBS, and sonicated in 0.5 mL NT-2 buffer. RIP conditions were as described (36, 37). Anti-m^7G cap antibody (5 μg) (MBL; RN016M) was coupled to 25 μL Sepharose G (GE Healthcare) beads per sample of 4 μg of RNA isolated from eIF4E-Flag or vector control cells.

Cap Quantitation. Denatured RNAs (10 μg) were treated with FastAP Thermosensitive Alkaline Phosphatase (Thermo Scientific) and purified using TRIzol and DirectZol miniprep columns. An aliquot of AP-treated RNAs was treated with T4 PNK (NEB) and purified as above. All RNAs were then treated with TAP (Enzymax), ligated to cap RNA linker using T4 single-stranded RNA ligase (NEB), and subsequently reverse-transcribed using random primers with specific overhang (60). Second-strand synthesis was performed using biotinylated primers matching the sequence from the cap RNA linker using High Fidelity Taq Polymerase (NEB). Biotinylated DNA strands were isolated using streptavidin-conjugated beads (Sigma) according to the manufacturer's recommendations, purified using a QIAquick PCR Purification Kit (Qiagen), and analyzed for selected transcripts by real-time PCR. A detailed protocol is described in *SI Appendix*.

RNA-Seq and Differential Gene Expression Analysis. Libraries were generated using a KAPA RNA HyperPrep with RiboErase Kit (Roche) following the manufacturer's instruction manual. All libraries were subjected to flow cell high-output (75 cycles) single-end sequencing on an Illumina NextSeq 500 sequencer at the Genomic platform of the Institute of Research in Immunology and Cancer, University of Montréal. Reads were aligned to the human reference genome (GRCh38.p5) using STAR (version 2.5.1b) (61). Detailed information is given in *SI Appendix*.

Data Availability. All study data are included in the article and *SI Appendix*, and the RNA-seq data have been deposited in the Gene Expression Omnibus (GEO) database (accession no. GSE158728).

ACKNOWLEDGMENTS. We are grateful for helpful discussions with Drs. Esterina D'Asti, Mehdi Ghram, and Gavin Morris. We thank Jennifer Huber and Raphaelle Lambert for help with RNA-seq experiments. K.L.B.B. acknowledges financial support from NIH R01 CA80728, NIH R01 CA98571, Canadian Institutes of Health Research PJT159785, Leukemia & Lymphoma Society USA Translational Research Program (LLS USA TRP) R6513-20, and the Canada Research Chair in Molecular Biology of the Cell Nucleus. L.C. acknowledges financial support from LLS USA TRP R6510-19 and M.V.R. acknowledges financial support from the Kellen Foundation and a Department of Medicine Postdoctoral Scholar Award.

1. V. H. Cowling, Regulation of mRNA cap methylation. *Biochem. J.* **425**, 295–302 (2009).
2. R. C. Pillutla, A. Shimamoto, Y. Furuichi, A. J. Shatkin, Human mRNA capping enzyme (RNGTT) and cap methyltransferase (RNMT) map to 6q16 and 18p11.22-p11.23, respectively. *Genomics* **54**, 351–353 (1998).
3. D. Varshney *et al.*, Molecular basis of RNA guanine-7 methyltransferase (RNMT) activation by RAM. *Nucleic Acids Res.* **44**, 10423–10436 (2016).
4. X. Mao, B. Schwer, S. Shuman, Yeast mRNA cap methyltransferase is a 50-kilodalton protein encoded by an essential gene. *Mol. Cell. Biol.* **15**, 4167–4174 (1995).
5. C. Fabrega, S. Hausmann, V. Shen, S. Shuman, C. D. Lima, Structure and mechanism of mRNA cap (guanine-N7) methyltransferase. *Mol. Cell* **13**, 77–89 (2004).
6. T. Gonatopoulos-Pournatzis, S. Dunn, R. Bounds, V. H. Cowling, RAM/Fam103a1 is required for mRNA cap methylation. *Mol. Cell* **44**, 585–596 (2011).
7. D. Varshney *et al.*, mRNA cap methyltransferase, RNMT-RAM, promotes RNA Pol II-dependent transcription. *Cell Rep.* **23**, 1530–1542 (2018).
8. C. Chu, A. J. Shatkin, Apoptosis and autophagy induction in mammalian cells by small interfering RNA knockdown of mRNA capping enzymes. *Mol. Cell. Biol.* **28**, 5829–5836 (2008).
9. B. Shafer, C. Chu, A. J. Shatkin, Human mRNA cap methyltransferase: Alternative nuclear localization signal motifs ensure nuclear localization required for viability. *Mol. Cell. Biol.* **25**, 2644–2649 (2005).
10. P. Srinivasan, F. Piano, A. J. Shatkin, mRNA capping enzyme requirement for *Caenorhabditis elegans* viability. *J. Biol. Chem.* **278**, 14168–14173 (2003).
11. D. R. Schoenberg, L. E. Maquat, Re-capping the message. *Trends Biochem. Sci.* **34**, 435–442 (2009).
12. Y. Otsuka, N. L. Kedersha, D. R. Schoenberg, Identification of a cytoplasmic complex that adds a cap onto 5′-monophosphate RNA. *Mol. Cell. Biol.* **29**, 2155–2167 (2009).
13. J. B. Trotman, A. J. Giltmier, C. Mukherjee, D. R. Schoenberg, RNA guanine-7 methyltransferase catalyzes the methylation of cytoplasmically recapped RNAs. *Nucleic Acids Res.* **45**, 10726–10739 (2017).
14. E. Grudzien-Nogalska, M. Kiledjian, New insights into decapping enzymes and selective mRNA decay. *Wiley Interdiscip. Rev. RNA* **8**, 10.1002/wrna.1379 (2017).
15. L. Davidson, A. Kerr, S. West, Co-transcriptional degradation of aberrant pre-mRNA by Xrn2. *EMBO J.* **31**, 2566–2578 (2012).
16. S. W. Liu *et al.*, Functional analysis of mRNA scavenger decapping enzymes. *RNA* **10**, 1412–1422 (2004).
17. K. V. Prasanth *et al.*, Regulating gene expression through RNA nuclear retention. *Cell* **123**, 249–263 (2005).
18. C. Girard *et al.*, Post-transcriptional spliceosomes are retained in nuclear speckles until splicing completion. *Nat. Commun.* **3**, 994 (2012).
19. A. P. Dias, K. Dufu, H. Lei, R. Reed, A role for TREX components in the release of spliced mRNA from nuclear speckle domains. *Nat. Commun.* **1**, 97 (2010).
20. V. H. Cowling, Myc up-regulates formation of the mRNA methyl cap. *Biochem. Soc. Trans.* **38**, 1598–1601 (2010).

21. V. H. Cowling, M. D. Cole, The Myc transactivation domain promotes global phosphorylation of the RNA polymerase II carboxy-terminal domain independently of direct DNA binding. *Mol. Cell. Biol.* **27**, 2059–2073 (2007).
22. M. D. Cole, V. H. Cowling, Specific regulation of mRNA cap methylation by the c-Myc and E2F1 transcription factors. *Oncogene* **28**, 1169–1175 (2009).
23. V. H. Cowling, Enhanced mRNA cap methylation increases cyclin D1 expression and promotes cell transformation. *Oncogene* **29**, 930–936 (2010).
24. S. Dunn, O. Lombardi, V. H. Cowling, c-Myc co-ordinates mRNA cap methylation and ribosomal RNA production. *Biochem. J.* **474**, 377–384 (2017).
25. F. Lejbkowicz *et al*., A fraction of the mRNA 5′ cap-binding protein, eukaryotic initiation factor 4E, localizes to the nucleus. *Proc. Natl. Acad. Sci. U.S.A.* **89**, 9612–9616 (1992).
26. F. J. Iborra, D. A. Jackson, P. R. Cook, Coupled transcription and translation within nuclei of mammalian cells. *Science* **293**, 1139–1142 (2001).
27. V. Lang, N. I. Zanchin, H. Lünsdorf, M. Tuite, J. E. McCarthy, Initiation factor eIF-4E of *Saccharomyces cerevisiae*. Distribution within the cell, binding to mRNA, and consequences of its overproduction. *J. Biol. Chem.* **269**, 6117–6123 (1994).
28. I. Topisirovic *et al*., Aberrant eukaryotic translation initiation factor 4E-dependent mRNA transport impedes hematopoietic differentiation and contributes to leukemogenesis. *Mol. Cell. Biol.* **23**, 8992–9002 (2003).
29. D. Rousseau, R. Kaspar, I. Rosenwald, L. Gehrke, N. Sonenberg, Translation initiation of ornithine decarboxylase and nucleocytoplasmic transport of cyclin D1 mRNA are increased in cells overexpressing eukaryotic initiation factor 4E. *Proc. Natl. Acad. Sci. U.S.A.* **93**, 1065–1070 (1996).
30. A. De Benedetti, A. L. Harris, eIF4E expression in tumors: Its possible role in progression of malignancies. *Int. J. Biochem. Cell Biol.* **31**, 59–72 (1999).
31. M. Carroll, K. L. Borden, The oncogene eIF4E: Using biochemical insights to target cancer. *J. Interferon Cytokine Res.* **33**, 227–238 (2013).
32. B. Culjkovic, I. Topisirovic, L. Skrabanek, M. Ruiz-Gutierrez, K. L. Borden, eIF4E is a central node of an RNA regulon that governs cellular proliferation. *J. Cell Biol.* **175**, 415–426 (2006).
33. B. Culjkovic, I. Topisirovic, L. Skrabanek, M. Ruiz-Gutierrez, K. L. Borden, eIF4E promotes nuclear export of cyclin D1 mRNAs via an element in the 3′UTR. *J. Cell Biol.* **169**, 245–256 (2005).
34. L. Volpon *et al*., A biochemical framework for eIF4E-dependent mRNA export and nuclear recycling of the export machinery. *RNA* **23**, 927–937 (2017).
35. I. Topisirovic *et al*., Molecular dissection of the eukaryotic initiation factor 4E (eIF4E) export-competent RNP. *EMBO J.* **28**, 1087–1098 (2009).
36. B. Culjkovic-Kraljacic *et al*., Combinatorial targeting of nuclear export and translation of RNA inhibits aggressive B-cell lymphomas. *Blood* **127**, 858–868 (2016).
37. H. A. Zahreddine *et al*., The eukaryotic translation initiation factor eIF4E harnesses hyaluronan production to drive its malignant activity. *eLife* **6**, e29830 (2017).
38. B. Culjkovic-Kraljacic, A. Baguet, L. Volpon, A. Amri, K. L. B. Borden, The oncogene eIF4E reprograms the nuclear pore complex to promote mRNA export and oncogenic transformation. *Cell Rep.* **2**, 207–215 (2012).
39. M. L. Truitt *et al*., Differential requirements for eIF4E dose in normal development and cancer. *Cell* **162**, 59–71 (2015).
40. A. Biswas, C. M. Brown, Scan for motifs: A webserver for the analysis of post-transcriptional regulatory elements in the 3′ untranslated regions (3′ UTRs) of mRNAs. *BMC Bioinformatics* **15**, 174 (2014).
41. E. Dassi *et al*., AURA 2: Empowering discovery of post-transcriptional networks. *Translation (Austin)* **2**, e27738 (2014).
42. V. Posternak, M. H. Ung, C. Cheng, M. D. Cole, MYC mediates mRNA cap methylation of canonical Wnt/β-catenin signaling transcripts by recruiting CDK7 and RNA methyltransferase. *Mol. Cancer Res.* **15**, 213–224 (2017).
43. R. J. Machida, Y. Y. Lin, Four methods of preparing mRNA 5′ end libraries using the Illumina sequencing platform. *PLoS One* **9**, e101812 (2014).
44. K. Maruyama, S. Sugano, Oligo-capping: A simple method to replace the cap structure of eukaryotic mRNAs with oligoribonucleotides. *Gene* **138**, 171–174 (1994).
45. J. E. Wilusz, Long noncoding RNAs: Re-writing dogmas of RNA processing and stability. *Biochim. Biophys. Acta* **1859**, 128–138 (2016).
46. R. Yoshimoto, A. Mayeda, M. Yoshida, S. Nakagawa, MALAT1 long non-coding RNA in cancer. *Biochim. Biophys. Acta* **1859**, 192–199 (2016).
47. I. Ulitsky, D. P. Bartel, lincRNAs: Genomics, evolution, and mechanisms. *Cell* **154**, 26–46 (2013).
48. L. Volpon *et al*., Importin 8 mediates m7G cap-sensitive nuclear import of the eukaryotic translation initiation factor eIF4E. *Proc. Natl. Acad. Sci. U.S.A.* **113**, 5263–5268 (2016).
49. C. Mukherjee *et al*., Identification of cytoplasmic capping targets reveals a role for cap homeostasis in translation and mRNA stability. *Cell Rep.* **2**, 674–684 (2012).
50. X. Jiao, J. H. Chang, T. Kilic, L. Tong, M. Kiledjian, A mammalian pre-mRNA 5′ end capping quality control mechanism and an unexpected link of capping to pre-mRNA processing. *Mol. Cell* **50**, 104–115 (2013).
51. X. Jiao *et al*., Identification of a quality-control mechanism for mRNA 5′-end capping. *Nature* **467**, 608–611 (2010).
52. S. K. Lim, L. E. Maquat, Human beta-globin mRNAs that harbor a nonsense codon are degraded in murine erythroid tissues to intermediates lacking regions of exon I or exons I and II that have a cap-like structure at the 5′ termini. *EMBO J.* **11**, 3271–3278 (1992).
53. K. L. B. Borden, L. Volpon, The diversity, plasticity, and adaptability of cap-dependent translation initiation and the associated machinery. *RNA Biol.* **17**, 1239–1251 (2020).
54. C. Klec, F. Prinz, M. Pichler, Involvement of the long noncoding RNA NEAT1 in carcinogenesis. *Mol. Oncol.* **13**, 46–60 (2019).
55. L. H. Schmidt *et al*., The long noncoding MALAT-1 RNA indicates a poor prognosis in non-small cell lung cancer and induces migration and tumor growth. *J. Thorac. Oncol.* **6**, 1984–1992 (2011). Correction in: *J. Thorac. Oncol.* **7**, 1206 (2012).
56. M. R. Davis, M. Delaleau, K. L. B. Borden, Nuclear eIF4E stimulates 3′-end cleavage of target RNAs. *Cell Rep.* **27**, 1397–1408.e4 (2019).
57. J. Yu *et al*., LncRNA SLCO4A1-AS1 facilitates growth and metastasis of colorectal cancer through β-catenin-dependent Wnt pathway. *J. Exp. Clin. Cancer Res.* **37**, 222 (2018).
58. V. Boivin *et al*., Simultaneous sequencing of coding and noncoding RNA reveals a human transcriptome dominated by a small number of highly expressed noncoding genes. *RNA* **24**, 950–965 (2018).
59. M. A. Diamantopoulos, P. Tsiakanikas, A. Scorilas, Non-coding RNAs: The riddle of the transcriptome and their perspectives in cancer. *Ann. Transl. Med.* **6**, 241 (2018).
60. M. Salimullah, M. Sakai, C. Plessy, P. Carninci, NanoCAGE: A high-resolution technique to discover and interrogate cell transcriptomes. *Cold Spring Harb. Protoc.* **2011**, pdb prot5559 (2011).
61. A. Dobin *et al*., STAR: Ultrafast universal RNA-seq aligner. *Bioinformatics* **29**, 15–21 (2013).